

Wide-Band Fading Channel Model for Micro-Cellular Systems

Ian Oppermann*, Benjamin White and Branka S. Vucetic

Dept. of Electrical Engineering, University of Sydney, NSW 2006, Australia

Abstract

This paper presents a model for a wide-band fading channel for terrestrial mobile applications. The model is based on the results of measurements made in a heavily built-up urban environment using a 25 MHz signal centred at approximately 2.6 GHz. This paper presents measured impulse responses and details the parameter extraction process used to determine the characteristics of the channel. These parameters are used in the channel simulation package and the output of these simulations are compared to the original data.

1 Introduction

Land mobile systems utilising micro-cellular techniques offer a great deal of flexibility for mobile users and offer the best hope of realising the desire of total personal communications networks. They allow for the provision of a wide range of services and offer communications in many different environments. Investigations of the performance of land-mobile communication is made more difficult by the complex nature of the channel. The signal is corrupted by noise, distorted by Doppler shifts and obstructed by both stationary and rapidly moving objects. Modelling this channel is vital in the design of communications systems to operate in this environment. Without an accurate model, the design process is made far more difficult and expensive.

This paper examines the radio frequency channel with a bandwidth of 25 MHz centered at 2.6 GHz associated with land mobile systems in heavily built-up urban environment. The model is characterised by a series of shadowed states and movement between these states is determined by a Markov process. This paper demonstrates that it is possible to model the channel with reasonable accuracy using the N-state, Markov channel model described in this paper.

2 Experimental Procedure

In order to determine the characteristics of a wide-band channel model which may be found in a micro-cellular system, an intensive series of measurements was carried out

[1] in a heavily built-up urban environment. The measurement procedure, described in [1], consisted of a continuously moving receiver taking impulse response readings from a stationary transmitter.

The transmitter consisted of a discone antenna mounted on a mast at a height of 10.4 metres and situated near a street intersection. The receiving antenna used was also a directional discone maintained at a height of 2.5 metres mounted on a vehicle travelling at an average of five kilometres per hour.

The road along which the measurements were taken was approximately 30 metres wide with smaller intersecting streets approximately 12 metres in width. The situation is similar to the environment described by Kukuskin [2]. The route considered was along one of the wider streets and, at one point, it crossed the road on which the base station antenna was located giving an unobstructed line-of-sight (LOS) for a short period. The remainder of the measurement period was characterised by heavy shadowing.

The measurement signal itself consisted of a spread spectrum signal with a spreading ratio of 511 and a chip duration of 40 ns. The received signal was sampled at approximately 50 M samples/sec to produce an impulse response profile every 3 cm. These measurements constitute the "Near" data. Figure 1 illustrates some of the received impulse response profiles for the experiment described above. The distance from the transmitter to the receiver for the "Near" measurements changed from approximately 100 metres to several 10's of metres. The profiles represent the signal after the noise has been reduced.

3 Channel Characteristics

In general, a multi-path fading channel may be represented in the base-band as a direct component and the sum of discrete signal components which vary in number, amplitude and phase [3], [4]. Each signal component is the result of propagation along a different path with different levels of attenuation and different delays relative to the component travelling along the LOS from transmitter to receiver [5], [6]. A generalised equation to represent the fading channel is given by [3]

$$c(\tau; t) = L(t)\delta(t) + \sum_n \alpha_n(t) \exp^{-j2\pi f_c \tau_n(t)} \delta[\tau - \tau_n(t)] \quad (1)$$

*This work was supported by the Australian Telecommunications and Electronics Research Board (ATERB)

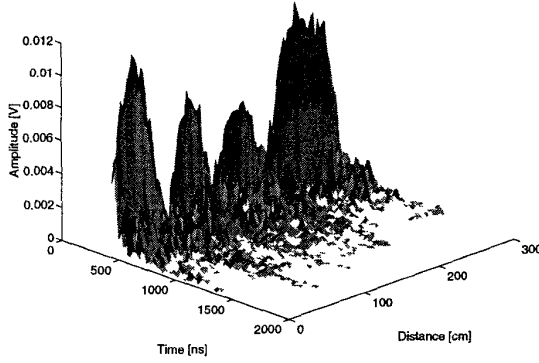


Figure 1: Impulse response Profiles After Removing Noise (Near Data)

where $L(t)$ is the time varying amplitude of the direct component, α_n is the time varying amplitude of the n th multi-path component, τ_i represents the delay of the i th multi-path component and f_c is the carrier frequency. The direct component may be Rayleigh, Rice or log-normal depending on the extent of obstruction of the LOS signal. The multi-path components will typically be Rayleigh, if no strong reflectors exist, Rician if some small number of strong reflectors exists, or Nakagami which covers many distributions between these two extremes [7], [8].

4 Parameter Extraction

It is known [3] that for small time durations the received multi-path, faded signal is highly correlated. It has also been observed [9] that a similar result holds for the level of correlation of the signal over small physical distances (of the order of 10's of wavelengths). For the purposes of extracting parameters for the model, the recorded waveform was divided into small sections called "windows". The data in each of these windows was considered to be highly correlated and so was treated as the output of a stationary random process.

Each window was initially categorised as either Rician or Shadowed depending on the variance of the mean signal envelope (the direct component variation). Rician states were further categorised depending on the Rician factor, K , the RMS value of the delay spread and the number of multi-path components. Shadowed states were categorised depending on the mean value of the signal envelope (direct component in this case), variance of the direct path envelope, number of multi-path components, RMS value of the delay spread and power of the multi-path components.

5 Channel Model

The model chosen to represent the wide-band channel is based on a linear, tapped-delayed, transversal filter (see

Figure 3) which mimics the physical processes described by Equation(1). This model however, must be capable of simulating significant changes in environment experienced by the receiver as it moves relative to the transmitter. This is done by modelling a finite set of states and causing the model to move between these states in a predetermined probabilistic manner. Similar to the narrow-band channel models implemented by Vucetic and Du [10], the model implements a Markov chain to achieve the state transitions. The transition probability matrix for an M state system is given in the form

$$P = \begin{bmatrix} p_{11} & p_{12} & \dots & p_{1M} \\ p_{21} & p_{22} & \dots & p_{2M} \\ \dots & \dots & \dots & \dots \\ p_{M1} & p_{M2} & \dots & p_{MM} \end{bmatrix} \quad (2)$$

where p_{ij} refers to the probability of the model changing from the current state i to the new state j . The matrix of state probabilities W is defined as

$$W = [W_1, W_2, \dots, W_M] \quad (3)$$

and must satisfy the conditions that

$$WP = W \quad (4)$$

$$WE = I \quad (5)$$

where E is a column matrix whose entries are 1's and I is the identity matrix.

Each of the data windows described in the Section above are allocated to one of the states being modelled. The parameters for each window are averaged in order to obtain a single set of parameters to define the final state. As a new state is entered, the model parameters are changed to adopt the characteristics of the new environment. The

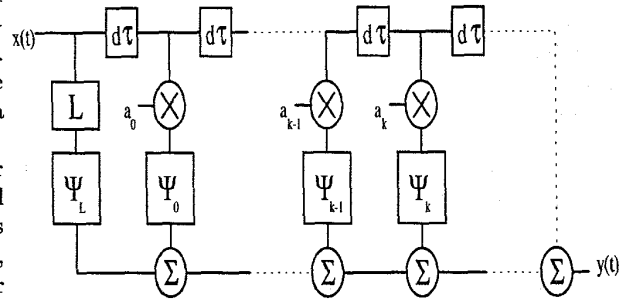


Figure 2: Fading Channel Model

number of branches in the model depends on the average number of multi-path components in the given state being modelled. Each branch also has a Doppler filter associated with it (as described in [9]). This has the effect of shaping the probability density function (pdf) of the particular multi-path component to that of the experimental response. The filter utilises the Doppler spectral information determined in the parameter extraction phase. Using

the filtering approach, it is a simple matter to change the distribution of the multi-path components depending on the state being modelled by specifying different Doppler spectra.

The direct component is capable of simulating both Shadowed (log-normal pdf) and Rician distributions. The Rician distribution is characterised by a mean envelope value (direct component value for impulse responses) and a variance for the high-frequency component of the direct signal. This high-frequency component consists of the Doppler shift of the direct component and the effect of any multi-path components which are not able to be resolved from the direct component.

The Shadowed distribution is characterised by a mean signal envelope, a fade rate associated with the frequency of occurrence of interfering objects, and a variance for the high frequency component of the direct component similar to the one described for the Rician state.

6 Simulation Results

Based on the extracted parameters, a series of impulse responses were generated for each state that was being modelled and compared to the experimentally obtained impulse responses. This Section presents both the results of the parameter extraction process and the comparison of the obtained impulse response components. For the purposes of simulation, six states were modelled. These consisted of one Rician state and two shadowed states with each of these states being further divided according to whether the state had a “large” or “small” value of RMS delay spread.

1 Parameter Values

The first process performed on the data was the separation of received impulse responses into states. For all parameters considered, the data from approximately 62 impulse response profiles was considered as a coherent signal and so the parameters of all impulses in each profile in a window were averaged to obtain values for the window.

Windows of data were classified as Rician states depending on the shape of the direct component. If the ratio of the variance to the square of the mean value (similar to the Rician factor for narrow-band waveforms) of the signal exceeded a given threshold (10 dB in this case), the window of data was classified as Rician. The Rician windows were divided according to whether they had long or short values of RMS delay spread with the threshold set at one microsecond. After this division, the parameters were averaged from all of the windows which had been classified in these states.

Windows which were not Rician were deemed to be shadowed states and were categorised depending on the mean value of the direct component. This produced a heavily shadowed state and a light shadowed state. After this stage, processing continued in a similar fashion to the Rician states. For the purposes of this Paper, the states are listed in order of Rice Short Delay, Rice Long Delay,

Table I: Rician State Average Parameters

State	Delay	Multi	Mean	K
	[μs]		[V]	[dB]
1	0.522	8	$12.5 \cdot 10^{-3}$	2.27
2	-	-	-	-

Table II: Shadowed State Average Parameters

State	Delay	Multi	Mean	σ_d	σ_m
	[μs]		[V]		
3	0.69	11	$2.1 \cdot 10^{-2}$	$1.1 \cdot 10^{-2}$	$2.6 \cdot 10^{-2}$
4	1.35	22	$6.5 \cdot 10^{-3}$	$3.7 \cdot 10^{-3}$	$6.8 \cdot 10^{-3}$
5	0.88	14	$5.2 \cdot 10^{-3}$	$2.2 \cdot 10^{-3}$	$5.6 \cdot 10^{-3}$
6	1.48	24	$5.1 \cdot 10^{-3}$	$2.6 \cdot 10^{-3}$	$5.5 \cdot 10^{-3}$

Light Shadowed Short Delay, Light Shadowed Long Delay, Heavy Shadowed Short Delay and Heavy Shadowed Long Delay.

This classification process resulted in state probabilities of

$$P = \begin{bmatrix} 0.200 & 0.000 & 0.600 & 0.200 & 0.000 & 0.000 \\ 0.000 & 0.000 & 0.000 & 0.000 & 0.000 & 0.000 \\ 0.235 & 0.000 & 0.411 & 0.058 & 0.176 & 0.117 \\ 0.230 & 0.000 & 0.000 & 0.538 & 0.000 & 0.230 \\ 0.000 & 0.000 & 0.000 & 0.000 & 0.500 & 0.500 \\ 0.058 & 0.000 & 0.235 & 0.117 & 0.000 & 0.588 \end{bmatrix} \quad (6)$$

The matrix of state probabilities was found to be

$$W = [0.161 \ 0.000 \ 0.274 \ 0.209 \ 0.080 \ 0.274] \quad (7)$$

From these results, it may be seen that the long RMS delay spread state for the Rician state is unpopulated.

From the transition matrix, it is possible to see that for most states, the most likely state transition is to return to the same state. Table I gives an overview of the parameters of the Rician states, while Table II gives the parameters for the shadowed states. The “Multi” column refers to the average number of multi-path components for the state. The columns headed M and σ_d refer to the mean value and standard deviation of the direct component amplitude, while σ_m refers to the RMS value of the multi-path component amplitudes. The Rician factor, K , for the Rician state may be calculated from the component terms of the direct and multi-path components.

$$K = \frac{M^2}{\sigma_d^2 + \sigma_m^2} \quad (8)$$

For simplicity, Table I simply lists the Rician factor. It should be noted that no power normalisation was performed on the data before parameters were extracted.

From these tables, it is possible to see that the direct component typically experiences interference from many multi-path components which have delay spreads of the order of 1 μs . These delay values vary quite significantly however, and the number of multi-path components changes almost proportionally. The power of the

multi-path components also found to decay exponentially, although not so rapidly as to remove the need to model the later components.

In order to determine the accuracy of the channel model, the parameters described above were used to generate a series of impulse responses and these were compared with the experimental data. The comparison was based on the probability density functions of the direct components and significant multi-path components of the various states. Figures 4 and 5 illustrate the pdf of the direct component, and first multi-path component of the impulse responses of data in the Rician State. Similarly, figures 7, 8 and 9 illustrate the pdf of the direct component, and first and third multi-path components of the impulse responses of the short RMS delay spread, heavily shadowed state.

From these figures, it is possible to see that in both Shadowed and Rician states, there is good agreement between the power and distribution of the simulated and experimental signal components.

7 Conclusions

Modelling the land-mobile channel is a highly complex process due to the rapidly changing nature of the medium and the many varying interference factors. The channel is characterised by heavy levels of shadowing and many multi-path components with delay spreads typically of the order of $1 \mu\text{s}$. The delay spread, however, has been shown to change quite significantly between states and therefore was used as a discriminating factor when categorising measured data into states.

This paper has introduced a wide-band channel model and simulator for modelling micro-cellular, land mobile environments. Using this model, it has been shown that it is possible to reproduce the measured baseband signal and therefore facilitate development of land mobile systems.

References

- [1] E. Moriyama, M. Mizuno, Y. Nagata, Y. Furuya, I. Kamiya and S. Hattori, "2.6 GHz band multipath characteristics for urban microcellular telecommunication systems" *42nd IEEE Vehicular Technology Society Conference*, Denver CO, No. 2, May 1992. pp 347-352.
- [2] A. Kukuskin, "Propagation Modelling in Mobile Communications", *A.T.R.*, Vol. 28, No 1, January 1994. pp 1 - 14.
- [3] J.G. Proakis, "Digital Communications", *McGraw Hill International Editions*, 2nd Edition, 1989. pp. 619-621.
- [4] M.J. Miller, B.S. Vucetic and L. Berry (Eds), "Satellite Communications: Mobile and fixed Services", *Kluwer Academic Publishers*, London, 1993.

- [5] T.S. Rappaport, S.Y. Seidel and R. Singh, "900-MHz Multi-path Propagation measurements for U.S. Digital Cellular Radiotelephone" *IEEE Transactions on Vehicular Technology*, Vol. 39, No. 2, May 1990. pp 132-139.
- [6] S.Y. Seidel, T.S. Rappaport, S. Jain, S. Lord and R. Singh, "Path Loss, Scattering, and Multi-path Delay Statistics in Four European Cities for Digital Cellular and Microcellular Radiotelephone" *IEEE Transactions on Vehicular Technology*, Vol. 40, No. 4, Nov 1992. pp 721-730.
- [7] Y. Hase, W.J. Vogel, J. Goldhirsh, "Fade-durations Derived From Land-Mobile-Satellite Measurements in Australia" *IEEE Transactions on Communications*, Vol. 39, No. 5, May 1991. pp. 664-668.
- [8] H. Hashemi, "The Indoor Radio Propagation Channel", *Proceedings of the IEEE*, Vol 81, No 7, July 1993. pp 943 - 968.
- [9] D.C. Cox, "Delay Doppler Characteristics of Multi-path propagation at 910 MHz in a Suburban Mobile radio Environment" *IEEE Transactions on Antennas and Propagation*, Vol. 40, No. 4, Nov 1992. pp 721-730.
- [10] B.S. Vucetic and J. Du, "Channel Modelling and Simulation in Satellite Mobile Communication Systems" *IEEE Journal On Selected Areas in Communications*,

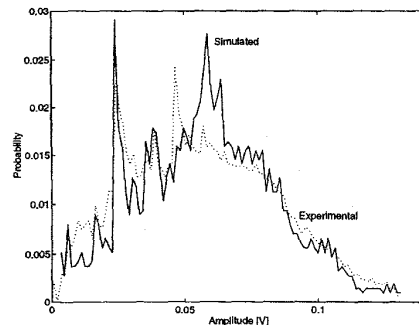


Figure 3: Rice State 1 Direct Component PDF

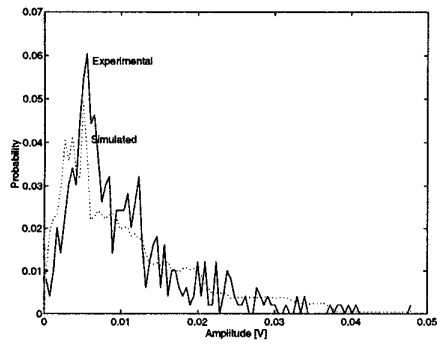


Figure 4: Rice State 1 First Multi-path PDF

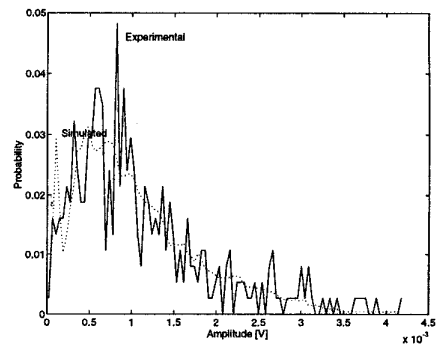


Figure 6: Shadowed State 3 Second Multi-path PDF

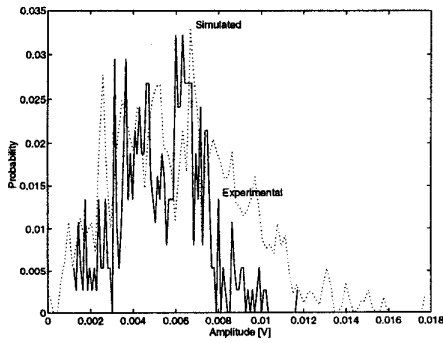


Figure 5: Shadowed State 3 Direct Component PDF

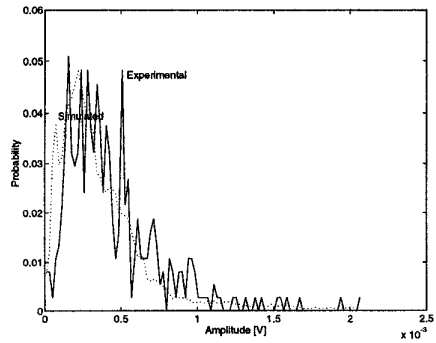


Figure 7: Shadowed State 3 Third Multi-path PDF